# First Principles Prediction of the Gas-Phase Precursors for AlN Sublimation Growth

Yanxin Li and Donald W. Brenner

*Department of Materials Science and Engineering, North Carolina State University, Raleigh, North Carolina 27695-7907, USA*

(Received 1 August 2003; published 18 February 2004)

Using a new, parameter-free first principles strategy for modeling sublimation growth, we show that while Al and $N_2$ dominate gas concentrations in AlN sublimation growth chambers under typical growth conditions, $N_2$ is undersaturated with respect to the crystal and therefore cannot be a growth precursor. Instead, our calculations predict that the nitrogen-containing precursors are $Al_nN$ ($n = 2, 3, 4$), in stark contrast to assumptions used in all previous modeling studies of this system.

DOI: 10.1103/PhysRevLett.92.075503 PACS numbers: 81.10.Aj, 81.05.Ea, 81.15.Aa

With applications that include photovoltaic detectors, optoelectronic field effect transistors, high frequency power devices, and light emitting diodes that can emit in the blue to near ultraviolet, nitride-based materials are revolutionizing twenty-first century solid-state microelectronics [1,2]. Because of the relatively close match between the lattice constants and thermal properties of AlN and GaN, AlN is typically used as a buffer layer for GaN-based devices where low defect structures are needed [1]. AlN is also a leading candidate to replace sapphire, Si, and SiC as a commercial substrate for nitride-based microelectronics applications [3–6]. In addition, the wide band gap of AlN (6.2 eV) can lead to $Al_xGa_{1-x}N$/AlN heterostructures with a wide range of tunable optoelectronic properties [1]. Sublimation deposition [7] is being used to produce relatively large size (about 1 $cm^2$) [6,8–10] and high quality (dislocation density $\sim 10^3$ $cm^{-2}$) [11] bulk AlN crystals at growth rates of about 0.50 mm/h [6,8]. In this technique material is transferred via sublimation from a high temperature, low-quality AlN solid to a lower temperature, higher-quality crystal under an isobaric $N_2$ gas environment. The main growth parameters are the inlet $N_2$ pressure $P_{N_2}$, the source temperature $T_s$, and the crystal temperature $T_c$ [8]. It has been determined empirically from experiment that manipulating these parameters, which presumably change the amounts and saturation state of gas-phase growth precursors, can alter the growth rate and crystal morphology [12]. Clearly, however, detailed relationships between growth precursors and growth conditions need to be more firmly established to optimize crystal production.

We present in this Letter a new, parameter-free first principles strategy for modeling sublimation growth that not only yields mole fractions of species in the gas phase as a function of reactor conditions, but also identifies growth precursors based on their degree of saturation with respect to the growing crystal. The strategy predicts that Al and $N_2$ dominate the species concentrations, in agreement with available experimental measurements [13], but that $N_2$ molecules are *undersaturated* with respect to the AlN crystal and therefore are unlikely growth precursors. Instead, our calculations predict that $Al_2N$, $Al_3N$, and $Al_4N$, while in smaller concentrations than $N_2$, are supersaturated and therefore are the main source of nitrogen contributing to AlN crystal growth. This first principles result is in stark contrast to all prior modeling studies, which start by assuming that Al atoms and $N_2$ are the growth precursors, and then account for isobaric reactor conditions via gas-phase transport effects using AlN vapor pressures due to sublimation in vacuum [7,9,10,14–16]. As discussed below, if the isobaric condition is applied to the calculation of both vapor pressure and transport effects, $N_2$ would be undersaturated at $T_c$ leading to no nitrogen-containing precursor in the gas phase under the two-species assumption.

Our modeling strategy considers two types of gaseous states. Both states are treated in an ideal gas approximation and are isobaric with one another in a typical sublimation chamber. The first state is a "boundary layer" (BL) that is sublimed from an AlN solid. It is used as a reference state for the gas in the vicinity of the source and the crystal for conditions under which there is no net sublimation or deposition. At a given temperature, the total aluminum content in all gaseous species is in equilibrium with the AlN solid, while the total nitrogen content is the sum of the nitrogen sublimed from the solid and any excess nitrogen from an external source needed to attain the isobaric condition. The second state is a "bulk gas" (BG) that spatially connects the source and crystal. We assume that for the BG, all aluminum in the aluminum-containing species comes from the source AlN due to sublimation at temperature $T_s$, and that all species within each isothermal layer of the BG are in local equilibrium [17] at the local gas temperature $T_g$. The total amount of Al atoms in all species is equal from one BG isothermal layer to another.

Comparing the mole fractions of species predicted in the BG with those predicted for the ideal crystal BL yields the saturation degree of each species. For a specific species, if its mole fraction in the BG is higher than that in the BL, the species is considered supersaturated, and it tends to deposit on the surface. In contrast, if the mole fraction of a species in the BG is lower than that in the BL, the species will tend to sublime from the crystal.

  

Our model emphasizes the saturation state of each gas-phase species and neglects mass transport effects. It is valid as long as local equilibrium is a good approximation. Some justification comes from analysis of the Knudson number for typical reactor conditions. For $P > 100$ torr, $T < 2300\,^{\circ}$C, species diameter $= 2.5$ Å, and a distance between the source and crystal $> 1$ mm, the Knudson number is less than 0.01, the threshold below which the assumption of local equilibrium is generally deemed acceptable.

A total of 16 gas-phase species of the form $Al_nN_m$ are considered in our model; these species correspond to $m = 0$, $n = 1$–3; $m = 1$, $n = 0$–4; $m = 2$, $n = 1$–4; and $m = 3$, $n = 0, 1$. Two of these species, $Al_2$ and AlN, have two spin multiplicities $S = 0, 1$; both are considered in the calculations. *Ab initio* binding energies and geometries calculated at various levels of theory, as well as limited thermodynamic data, are available for some of these species. However, a complete set of thermodynamic data as a function of temperature is unavailable. Therefore thermodynamic properties for these species were generated from statistical chemical equilibrium calculations [18] using energies, vibrational frequencies, and rotational moments of inertia generated from *ab initio* calculations using GAUSSIAN-98 [19]. After systematic trial computations involving various density functionals and composite Hartree-Fock theories, the details of which will be given elsewhere, it was determined that B3PW91/Aug-cc-pVTZ plus frequency analysis calculations provide the highest overall accuracy for all species considered based on comparisons to available experimental values of $\Delta H_f^0$ (298 K). In terms of enthalpy, the maximum relative deviation from the available experimental values is 12.5%, and the root-mean-square of the relative deviation is 3.9% for a larger set of 43 species containing chemical bonds between metal-metal, metal-nonmetal, and nonmetal-nonmetal atoms. The atomic energies of Al and N in the output of the calculation are further calibrated based on the JANAF tables [13] to have a correct relative energy between Al and N atoms.

To calculate concentrations under local equilibrium, we require that each species satisfies the relation

$$\mu_{Al_nN_m}(T, P_{Al_nN_m}) = n\mu_{Al}(T, P_{Al}) + m\mu_N(T, P_N), \quad (1)$$

where $\mu_i(T, P_i)$ is the chemical potential of species $i$ with partial pressure $P_i$. This yields 14 independent equations among the 16 gaseous species. Therefore two more constraints are needed to completely determine all mole fractions. The constraints are the isobaric conditions in a sublimation chamber

$$\sum_{Al_nN_m} P_{Al_nN_m} = P_{\text{total}} \quad (2)$$

and the stoichiometry condition

$$\sum_{Al_nN_m} (m - n)P_{Al_nN_m} = \begin{cases} 2(P_{\text{total}} - P_v); \\ 0; \quad \text{if } P_{\text{total}} \le P_v, \end{cases} \quad (3)$$

where the sums are over all species, $P_{Al_nN_m}$ is the partial pressure of species $Al_nN_m$, and the quantity $P_v$ is the saturated vapor pressure available from the JANAF tables [13]. The latter is a function of $T_s$ and $T_g$ for the BG, and of $T_s$ or $T_c$ for the BLs. The left-hand side of Eq. (3) is the excess amount of nitrogen beyond a 1:1 stoichiometry. If $P_{\text{total}} < P_v$, the inlet $N_2$ is unable to dilute the sublimed vapor, and in this case the right side of Eq. (3) constrains the vapor to a 1:1 stoichiometry. For $P_{\text{total}} > P_v$ the right-hand side of Eq. (3) ensures that the pressure of the extra nitrogen originates from the inlet $N_2$. In a latter part of this Letter calculations of the saturation state of species above pure Al are presented. These calculations use Eqs. (1)–(3) where $P_v(T)$ is the saturated vapor pressure of liquid Al published in the JANAF tables [13].

The calculated mole fractions for each of the species are plotted in Fig. 1 for a typical set of experimental growth conditions. The dashed lines indicate the mole fractions in a BG subliming from the source at $T_s$ and as a function of $T_g$. The solid curves correspond to mole fractions in a BL as a function of surface temperature. At the source temperature the two sets of mole fractions are identical by definition in our model but deviate from one another as the source and crystal temperatures become different. The calculations predict that Al and $N_2$ are the most abundant species in the typical temperature and pressure range for AlN growth. This is in agreement with limited experimental measurements of vapor pressures above an AlN crystal [20–22] and previous growth models [7,9,10,14–16] in which only Al and $N_2$ are considered. However, the mole fraction for $N_2$ in the BG is

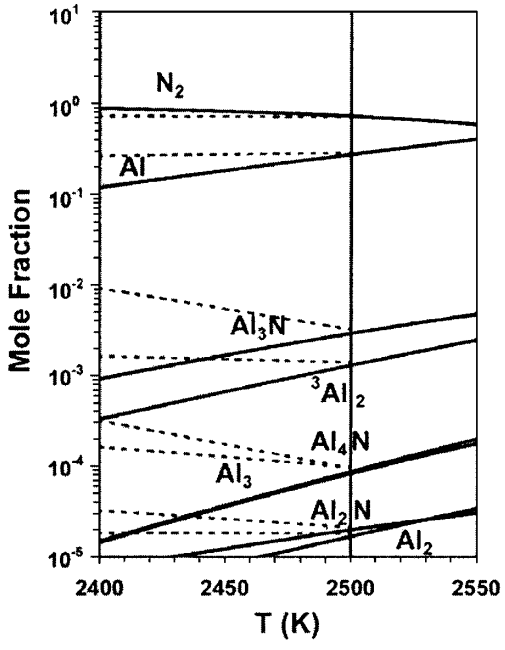


FIG. 1. Calculated mole fractions for AlN sublimation growth calculated at $P_{N_2} = 400$ torr. The solid lines are for the BL of an AlN surface, and the dashed lines are for the BG sublimed at $T_s = 2500$ K (denoted by the vertical line).

lower than that for the BL for all crystal temperatures below that of the source. As discussed above, this result indicates that $N_2$ is *undersaturated* with respect to the crystal and is therefore *not* a growth precursor.

The calculated concentration distributions in Fig. 1 can be explained in terms of species stability. The mole fractions of $Al_nN$ ($n = 2, 3, 4$) satisfy $X_{Al_2N} < X_{Al_4N} < X_{Al_3N}$. The relation $X_{Al_2N} < X_{Al_3N}$ is due to the strong covalent bonding between the $sp^2$ electrons of nitrogen and the $3p$ electron of aluminum. Because the Al-N bond in the planar $Al_4N$ is not as strong as that in the planar $Al_3N$, the energy gain for $Al + Al_3N \rightarrow Al_4N$ is not able to balance the entropy loss, leading to its concentration being between that for the species $Al_2N$ and $Al_3N$. Similarly, the relation $X_{Al_3} < X_{Al_2} < X_{Al}$ reflects that the weak metallic bonding among Al atoms is not sufficiently strong to balance the entropy loss. In addition, the mole fraction of $^3Al_2$ is higher than that of $Al_2$, reflecting the nonlocal, or metallic, character of electrons in $Al_2$.

As stated above, $N_2$ is calculated to be undersaturated with respect to the crystal and therefore cannot be a growth precursor. However, the other nitrogen-containing species $Al_nN$, $n = 2$–4, while in smaller concentrations, are supersaturated and therefore are possible candidates for growth precursors provided that they are in sufficient abundance to produce reasonable growth rates. Assuming that the rate-limiting step is nitrogen incorporation into the lattice, the growth rate contributed by each species can be estimated at a temperature $T$ from the Hertz-Knudsen-Langmuir equation [14]. The calculated results are given in Table I (assuming unit sticking coefficients) for growth of a wurtzite crystal along the $c$ direction for the source temperature indicated by the vertical line in Fig. 1 (2500 K) and a crystal temperature of 2440 K. The absolute concentrations of $Al_nN$ ($n = 2, 3, 4$) are predicted to be adequate to generate the measured growth rates, supporting our prediction that the $Al_nN$ species are the nitrogen-containing growth precursors. In agreement with Dreger's experimental conclusion that the ratio of sticking coefficient for N to Al should be close to unity [21], these species yield a ratio between 0.25 and 0.5 for $n = 2, 3, 4$. For comparison, prior modeling studies, all of which have assumed that $N_2$ is the growth precursor, have had to use a small ratio of $N_2$ to Al sticking coefficients on the order of $10^{-5}$–$10^{-3}$ to reproduce experimental growth rates [9,10,14–16].

The undersaturation of $N_2$ can be simply understood by considering the difference in pressure behavior as a function of temperature in the BL, which is given by the JANAF tables, and the ideal gas behavior of the BG. Under typical growth conditions the temperature decreases ~60 K from the source to the crystal. Assuming a typical source temperature $T_s \sim 2500$ K [8], according to the JANAF tables the vaporization pressure in the BLs exponentially decreases about 39%, from 163.3 to 99.56 torr [13]. Over the same temperature drop the pressure of the sublimated gaseous species in the BG linearly decreases by $1 - T_c/T_s = (1 - 2440/2500)$, or only about 2.4%. Under an isobaric environment of 400 torr, the BL at the crystal surface therefore contains a much larger fraction of inlet $N_2$ (about 39%) than the BG (about 2.4%), leading to a lower concentration of $N_2$ in the BG than that in the BL. Therefore $N_2$ tends to leave the BL rather than being deposited onto the crystal.

Aluminum-rich growth precursors for nitrogen incorporation together with the supersaturated state of aluminum atoms above the AlN crystal predicted by our model raises the issue if liquid aluminum formation is more favorable than AlN during growth. To explore this issue, we have calculated BL mole fractions above pure aluminum for the sublimation growth conditions considered above assuming a BG originating from an AlN source. The resulting mole fractions of the BG and the BL above pure aluminum (which is a liquid at this temperature) as a function of temperature are plotted in Fig. 2. For aluminum within about 60 K of the source temperature, aluminum atoms are undersaturated and $N_2$ molecules are supersaturated with respect to the liquid aluminum crystal, suggesting that the thermodynamics of the system drives the crystal away from an aluminum rich stoichiometry toward AlN. For larger temperature differences, the mole fraction curves are reversed and deposition of Al atoms from the BG is thermodynamically favored. However, the BL associated with the liquid aluminum is supersaturated with respect to an AlN BL for all aluminum-containing species, suggesting that any liquid aluminum formed in the reactor is unstable compared to AlN. Therefore for $\Delta T = T_s - T_c > 60$ K, transient liquid aluminum precipitation is an additional thermodynamically favorable path to form an AlN crystal from an AlN BG.

The results of several recent experiments have provided indirect evidence that $Al_nN_m$ species may play a role in the deposition of AlN [23–25]. In an experiment by Andrews *et al.* [23], for example, Al atoms produced by laser ablation of bulk aluminum was reacted with $N_2$, and the products condensed to 10 K on a CsI window. Infrared spectroscopy, supported by *ab initio* calculations, identified several trapped $Al_nN_m$ species, including relatively large concentrations of $Al_2N$ and $Al_3N$. According to the

TABLE I. Evaluation of $Al_nN$ significance to AlN growth.

| $T = T_c = 2440$ K, $P_{N_2} = 400$ torr | $Al_2N$ | $Al_3N$ | $Al_4N$ | Expt. [8] |
|---|---|---|---|---|
| Mole fraction difference $\Delta X_i$ | $1.8 \times 10^{-5}$ | $5.1 \times 10^{-2}$ | $2.2 \times 10^{-3}$ | |
| Growth rate (cm/h) | 0.046 | 11 | 0.43 | $> 0.054$ |

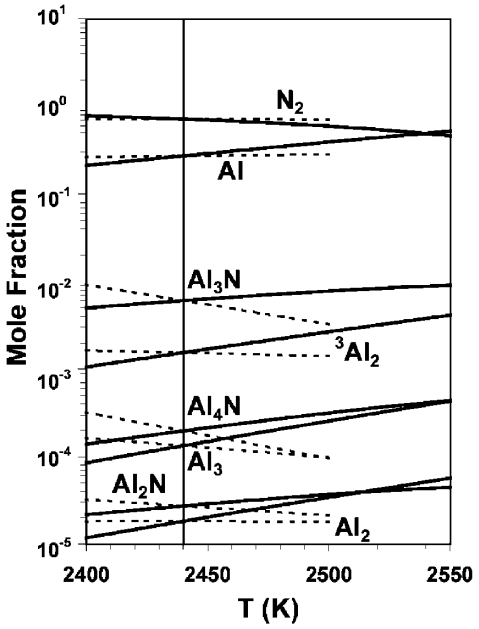


FIG. 2. Predicted gaseous mole fractions for pure aluminum as the "crystal" under the same conditions as in Fig. 1. The solid curve corresponds to a BL above the pure liquid aluminum. The dashed curve is the same as in Fig. 1.

authors, their work "provides the first experimental evidence for molecular species $Al_xN_y$ that may be involved in ceramic film growth." In related work, Leskiw and Castleman used mass spectrometry to characterize $Al_nN_m^-$ clusters produced by vaporizing an Al rod in the presence of an inert carrier gas and a small percentage of nitrogen [26]. They reported that $Al_nN^-$ clusters are the most abundant species measured.

In light of the above theoretical results, it is of interest to reexamine the experimental basis supporting the two-species assumption used in prior modeling studies. The original basis for this assumption can be traced through the JANAF tables [13] back to a mass spectrometry study of solid AlN vaporization by Schissel and William (SW), who reported only the presence of Al and $N_2$ [20]. It appears that in later studies [21,22] their assertion that no other species are present was assumed correct, and we cannot find any additional experiments carried out to further probe this assertion. We have two concerns with the two-species assumption. First, SW's heat of formation was reported to two significant figures (63 kcal/mol) implying a relative error in their measurement of about $0.5 \times 10^{-2}$. Based on our results, the mole fraction of other $Al_nN_m$ species would be below their experimental threshold for detecting these species. Second, in subsequent experimental measurements it was assumed that the dominant heterogeneous gaseous species would be AlN [21,22]. Based on $X_{Al_2N} < X_{Al_4N} < X_{Al_3N}$, gaseous AlN is predicted as the least stable species in the family of AlN, $Al_2N$, $Al_3N$, and $Al_4N$, and its mole fraction in Fig. 1 is so small ($< 10^{-5}$) that it does not significantly contribute to the gas environment. This explains why efforts to experimentally detect $Al_nN$ ($n = 2, 3, 4$) have been successful [23–26], while the existence of AlN is still controversial [27]. Hence an absence of gaseous AlN cannot be taken as evidence for the absence of other $Al_nN_m$ heterogeneous species.

The authors thank Z. Sitar, R. Schlesser, and R. Dalmau for helpful discussions and J. David Schall for critically reading this manuscript. This work was funded by the Office of Naval Research through MURI Contract No. N00014-01-1-0302 and by the North Carolina Super Computing Center.

[1] S. N. Mohammad, A. A. Salvador, and H. Morkoc, Proc. IEEE **83**, 1306 (1995).
[2] F. A. Ponce and D. P. Bour, Nature (London) **386**, 351 (1997).
[3] J. C. Rojo *et al.*, J. Cryst. Growth **231**, 317 (2001).
[4] R. Schlesser and Z. Sitar, J. Cryst. Growth **234**, 349 (2002).
[5] L. Liu and J. H. Edgar, Mater. Sci. Eng., R **37**, 61 (2002).
[6] N. B. Singh *et al.*, J. Cryst. Growth **250**, 107 (2003).
[7] G. A. Slack and T. F. McNelly, J. Cryst. Growth **34**, 263 (1976).
[8] R. Schlesser, R. Dalmau, and Z. Sitar, J. Cryst. Growth **241**, 416 (2002).
[9] S. Y. Karpov *et al.*, Phys. Status Solidi A **176**, 435 (1999).
[10] A. S. Segal *et al.*, J. Cryst. Growth **211**, 68 (2000).
[11] B. Raghothamachar *et al.*, J. Cryst. Growth **246**, 271 (2002).
[12] D. A. Porter and K. E. Easterling, *Phase Transformations in Metals and Alloys* (Van Nostrand Reinhold Co. Ltd., Workingham, England, 1981).
[13] M. W. Chase, Jr., *NIST-JANAF Thermochemical Tables* (ACS and AIP, Woodbury, NY, 1998).
[14] P. M. Dryburgh, J. Cryst. Growth **125**, 65 (1992).
[15] L. Liu and J. H. Edgar, J. Cryst. Growth **220**, 243 (2000).
[16] L. Liu and J. H. Edgar, J. Electrochem. Soc. **149**, G12 (2002).
[17] D. Kondepudi and I. Prigogine, *Modern Thermodynamics: From Heat Engines to Dissipative Structures* (John Wiley, New York, 1998).
[18] D. A. McQuarrie, *Statistical Mechanics* (Harper & Row, New York, 1976).
[19] M. J. Frisch *et al.*, *Gaussian 98 (Revision A.1x)* (Gaussian, Inc., Pittsburgh, PA, 2001).
[20] P. O. Schissel and W. S. Williams, Bull. Am. Phys. Soc. **4**, 139 (1959).
[21] L. H. Dreger, V. V. Dadape, and J. L. Margrave, J. Phys. Chem. **66**, 1556 (1962).
[22] D. L. Hildenbrand and W. F. Hall, J. Phys. Chem. **67**, 888 (1963).
[23] L. Andrews *et al.*, J. Phys. Chem. A **104**, 1656 (2000).
[24] G. Meloni and K. A. Gingerich, J. Chem. Phys. **113**, 10978 (2000).
[25] S. K. Nayak *et al.*, Chem. Phys. Lett. **301**, 379 (1999).
[26] B. D. Leskiw and J. A. W. Castleman, J. Chem. Phys. **114**, 1165 (2001).
[27] J. Hermann and C. Dutouquet, J. Appl. Phys. **91**, 10188 (2002).